

ENERGY SPECTRUM OF NUCLEAR-ACTIVE PARTICLES IN EXTENSIVE AIR SHOWERS

Kh. P. BABAYAN, N. G. BOYADZHIAN, N. L. GRIGOROV, É. A. MAMIDZHANYAN,
Ch. A. TRET'YAKOVA, and V. Ya. SHESTOPEROV

Nuclear Physics Institute, Moscow State University; Physics Institute, Academy of
Sciences, Armenian S.S.R.

Submitted to JETP editor February 15, 1963

J. Exptl. Theoret. Phys. (U.S.S.R.) 45, 418-427 (September, 1963)

Ionization bursts produced by nuclear-active particles in extensive air showers were studied using an array of 192 ionization chambers with a total area of 10 m^2 . It was found that the ionization burst spectrum differs from the spectrum of nuclear-active particles because of the simultaneous incidence of several nuclear-active particles upon the large-area array. The power exponent of the integral burst spectrum over an area of 10 m^2 in showers with more than 10^5 particles is $\gamma \sim 1.0$ (for bursts containing more than 500 relativistic particles), whereas the spectrum exponent for bursts produced by single particles in the same showers is $\gamma = 1.6 \pm 0.1$.

INTRODUCTION

NUMEROUS experiments^[1-3] were undertaken in recent years to measure the spectrum of nuclear-active particles in extensive air showers (EAS). The interest in the subject is due to the fact that the energy spectrum of nuclear-active particles constitutes one of the most essential characteristics of EAS. Using the data on the spectrum of nuclear-active particles we can estimate the energy of the nuclear-active component of EAS and, consequently, determine its role in the shower development. Moreover, it is especially interesting to study the nuclear-active particles in the high-energy range ($E \geq 10^{11}$ – 10^{12} eV) since from the knowledge of the number of high-energy particles in the shower we can draw definite conclusions concerning the mechanism of development of EAS.

In the experiments mentioned above^[1,2] the nuclear-active particles with energy greater than 10^{11} eV were studied by means of ionization chambers having an area of the order of 1 m^2 and more. The quantity measured was the spectrum of ionization bursts produced by nuclear-active particles in EAS, which was then recalculated to obtain the spectrum of nuclear-active particles. It was found that in a large energy interval (from $\sim 10^{11}$ to $\sim 10^{13}$ eV) the integral spectrum exponent of nuclear-active particles in EAS is close to unity, and is practically independent of the shower size. Thus, e.g., Vernov et al^[1] have concluded that the integral spectrum of nuclear-active particles in

the energy range $E \geq 10^{12}$ eV (the authors consider that the particles with energy $E \geq 10^{12}$ eV produce in the array a burst greater than 10^3 particles) in EAS with the size between 2×10^4 and 5×10^5 particles has an exponent $\gamma = 1.0 \pm 0.2$. Dovzhenko, Zatsepin, et al^[2] found that for energies from 10^{11} to 10^{12} eV the spectrum exponent is $\gamma = 0.9 \pm 0.1$, and at large energies increases to 1.3–1.4.

Since the experiments were carried out using large-area arrays it cannot be precluded, as mentioned by the authors themselves (see e.g. ^[2]), that in a number of cases, especially in those associated with large bursts, several nuclear-active particles fell simultaneously upon the array, which caused the distortion of the measured spectrum of nuclear-active particles. In our previous articles^[4,5] we have shown that, when detecting large ionization bursts using an array with an area of the order of several square meters, very often several nuclear-active particles fall simultaneously on the array. This effect leads to a considerable difference between the spectrum of the nuclear-active particles and the spectrum of the bursts produced by them in the array. Thus, the spectrum of bursts detected over an area of 10 m^2 has an exponent $\gamma = 1.38 \pm 0.03$ (for bursts greater than 2×10^3 particles), while the spectrum of nuclear-active particles has an exponent $\gamma = 1.92 \pm 0.05$.

It is reasonable to expect that when detecting EAS, and especially their core region, a considerable number of bursts is produced by a simultaneous incidence upon the array of several nuclear-active particles. The spectrum of bursts recorded

by large-area arrays may therefore differ considerably from the true spectrum of nuclear-active particles in EAS.

The size of the array detecting the bursts should therefore be sufficiently small to ensure that the burst spectrum will coincide with the spectrum of the nuclear-active particles. On the other hand, the total area of the nuclear-active particle detectors should be sufficiently large to achieve good statistical accuracy. Our array satisfied both these requirements, and enabled us to reduce considerably the systematic errors in the determination of the spectrum of nuclear-active particles due to a simultaneous incidence of several nuclear-active particles upon the array.

EXPERIMENTAL ARRANGEMENT

The study of the nuclear-active particles in EAS was carried out at sea level (Moscow) and at an altitude of 3200 m above sea level, using arrays with a working area of 10 m^2 .

The diagram of the array operating at 3200 m and the principle of its operation were described earlier.^[5] The array consisted of six layers of ionization chambers, 330 cm long and 10 cm in diameter each. Each layer consisted of 32 such chambers. The two upper layers of chambers, placed under lead absorbers 2 and 3 cm thick, respectively, served to detect the electron-photon component reaching the array from the air, and to measure its energy. The following four layers, placed under composite graphite-lead absorber, detected the nuclear-active particles. The thickness of the graphite absorbers was 60 g/cm^2 (upper absorber) and 210 g/cm^2 (lower absorber). It should be mentioned that our earlier analysis^[5] showed that a part of the ionization bursts recorded by the chambers underneath the graphite absorbers was due to soft component particles, propagating at large angles to the vertical and entering the array from the side. This effect was especially strongly felt for the two lower layers of chambers, placed under a 210 g/cm^2 graphite absorber. In order to select only the bursts due to nuclear-active particles, we used only the data of the chambers placed under the 60 g/cm^2 graphite absorber.

In the array operating at sea level there was one graphite absorber 60 g/cm^2 thick. A diagram of the array is given in ^[4].

Each ionization chamber was connected to a separate amplifier with a dynamic range corresponding to the passage through the chamber of 200 to $\sim 70,000$ relativistic particles. The values of ionization bursts in the following are not cor-

rected for the lead-brass transition effect which, according to ^[6], amounts in our case to 1.4.

At 3200 m above sea level, about 50% of the time the array operated in conjunction with a Geiger-counter hodoscope. The counters with an area of 330 cm^2 each were placed at six points at distances from 1 to 10 m from the center of the array. Each group consisted of 12 counters. The hodoscope served to measure the shower size in the range from 10^4 to 3×10^5 particles.

The array operated whenever the ionization was greater than a given value in two or more chamber layers. During the work at the mountain altitude, the threshold for the two upper chamber layers, which detected the electron-photon component from the air, was equivalent to the ionization produced by 8500 particles, and for the lower rows, which detected the nuclear-active particles, to that of 2400 particles. At sea level, the corresponding values were equal to 2400 and 1200 respectively.

Since the intensity of EAS at the altitude of 3200 m is 10 times greater than at sea level, the main part of the experimental data were obtained in the mountain altitude run. Greater attention is therefore paid to the data obtained at the altitude of 3200 m above sea level.

RESULTS

1. Selection of events. EAS were selected mainly by the two upper layers of ionization chambers placed under a thin lead absorber. It is known that the mean energy of electrons and photons in the central part of EAS (at distances up to 10 m from the shower axis) is of the order of 3×10^8 to 3×10^9 eV.^[8] The electrons and photons of such an energy produce in the lead cascade showers with the maximum of development at a depth of 4 to 5 radiation lengths, i.e., just at the level of the two upper chamber rows. Therefore, whenever the central part of an EAS fell upon the array, we could determine from the readings of the upper chamber layers the energy of the electron-photon component incident upon the array.

From the experimental data on the lateral distribution of the energy flux of the electron-photon component in EAS it follows that whenever the axis of a shower of 10^5 particles fell upon the center of our 10 m^2 array, the energy of the electron-photon component incident upon the array amounted to 2×10^{12} eV at 3200 m above sea level, and to 2.6×10^{12} eV at sea level (the difference in the energy is due to the difference in the air density at the corresponding altitudes). Moreover, at the altitude

of 3200 m, about 20,000 particles were present at the cascade maximum in the upper lead absorber, but because of the lead-brass transition effect,^[6] 1.4 times less particles passed through the upper layers, i.e., $\sim 1.4 \times 10^4$ particles. In order to select EAS with $N \gtrsim 10^5$ we chose therefore the events in which the size I_{ep} of the burst in at least one of the upper chamber layers was greater than 1.2×10^4 particles. In addition, we required the distribution of the ionization in the chambers of both upper layers to have a maximum in the central part of the array, not closer than 20 cm to its edge. An example of a selected event is shown in Fig. 1, where we can see the distribution of the ionization among the chambers of the upper layers, and the layers below the 60 g/cm² graphite absorber. We detected 596 such events during 713 hours of operation at 3200 m and 128 events during 1840 hours of operation at sea level.

The majority of selected events were showers with size greater than 10^5 particles with the axis incident upon the array. In a number of cases, however, a large burst in the upper layers of the chambers could have been produced also by showers having less than 10^5 particles, but with a steeper than average distribution of the electron-photon component. The indications of the hodoscope were used to find the shower size in the selected events, and also what fraction of EAS with $N \geq 10^5$ was included in our data.

2. Hodoscope operation and the relation between the burst size in the upper chamber layers and the shower size. As already mentioned, the array operated in conjunction with a hodoscope consisting of several counter trays during a part of the time. During the concurrent operation of the array and of the hodoscope, 431 coincidence events were detected in which the axis of an EAS fell upon the array and the burst size in the upper chamber layers was greater than 1.2×10^4 particles. For each of these events we found the number of particles in the shower from the hodoscope readings. It was assumed that the lateral distribution function of charged particles in the central part of the shower at distances smaller than 10 m from the shower axis is $\rho(r) = ANr^{-1}$, where $A = 1.5 \times 10^{-3}$,^[8] and that the shower axis coincides with the point of intersection of the chambers of the two upper layers, which recorded maximum ionization.

The reduction of the data showed that practically all selected events (more than 90%) were due to EAS with a size greater than 10^4 particles. 70% of the events were due to the incidence of showers with more than 10^5 particles. Thus, using the above method, we selected effectively EAS with $N > 10^5$.

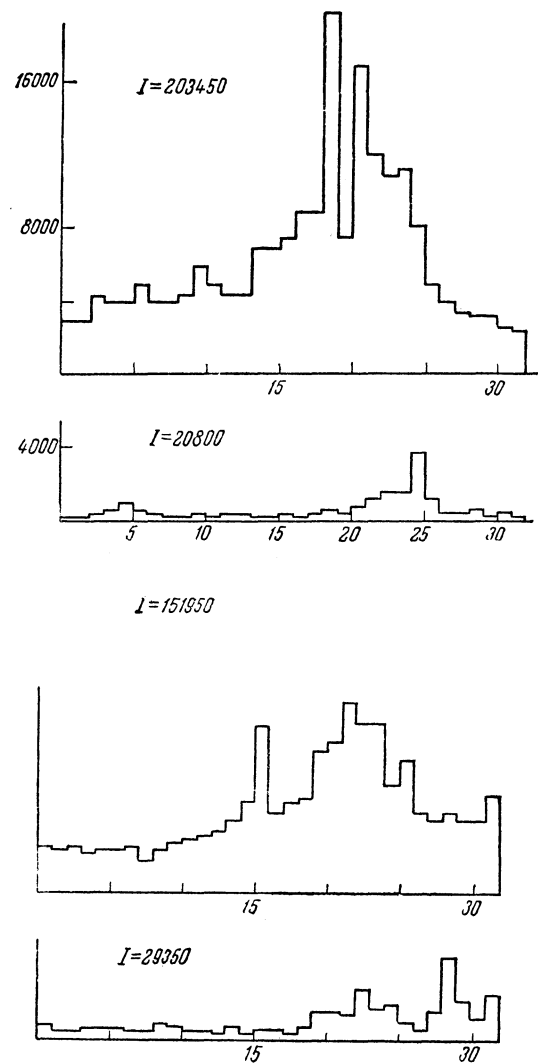


FIG. 1. An example of the ionization distribution among the chambers of the upper layers (upper histograms) and the layers underneath the 60 g/cm² graphite absorber, in an event in which the shower core fell upon the array. The x axis represents the chamber in a given layer, and the y axis the ionization in the chamber expressed in the number of particles traversing the chamber. I—total ionization in a given chamber layer.

For the subsequent analysis it is necessary to establish what fraction of EAS with $N > 10^5$ particles was included in the data. It is possible that a fraction of showers of a given size having a relatively small energy of the electron-photon component was excluded from our analysis, and that the results obtained refer therefore to a special class of EAS in which the electron-photon component has special energy characteristics, different from the average.

In order to answer this question we constructed the integral size spectrum of the detected showers, which is shown in Fig. 2. The x axis represents the shower size determined by the hodoscope, and

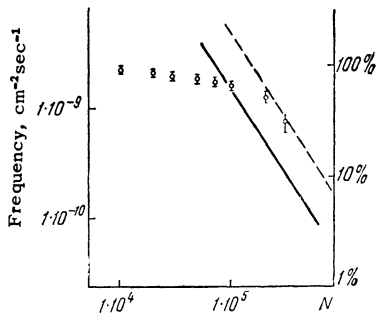


FIG. 2. Size spectrum of detected showers.

the y axis the experimental detection frequency of the cores of EAS with sizes greater than N . The right-hand scale represents the percentage of showers with a size greater than N among all the selected events. The integral size spectra of EAS obtained by Chudakov et al.^[9] (solid line) and Kameda et al.^[10] (dotted line), normalized to an observation level of 3200 m above sea level, are also shown in the figure. A comparison of the frequency of the selected showers with $N \geq 10^5$ with the absolute frequency of such showers determined in^[9,10] reveals that using our method of shower selection based on the readings of the upper rows of ionization chambers we detect practically all showers with $N \geq 10^5$ whose axes fall upon our array.

Among the selected events there is, nevertheless, a small percentage of showers smaller than 10^5 particles. Evidently, in those showers the lateral distribution function of the energy flux of the electron-photon component is considerably steeper than on the average. Since in the earlier experiments (e.g.,^[1,2]) it has been established that the spectrum of nuclear-active particles in EAS is practically independent of the shower size, we can expect that the showers with $N < 10^5$ do not essentially affect the results obtained.

The average size of the showers which produced bursts from 1.2×10^4 to 2.4×10^4 particles in the upper chamber layers was found to equal $\bar{N} = 1.34 \times 10^5$ (\bar{N} was determined from 108 events). Since the mean burst size in the range from 1.2×10^4 to 2.4×10^4 particles is 1.65×10^4 particles, we can consider that the selected events, for which the burst size in the upper layers was equal to I_{ep} , were due to EAS of an average size $\bar{N} \approx 10 I_{ep}$. We assume that the relation between the mean shower size and the bursts produced in the upper chamber layers remains true for bigger showers, since the lateral distribution function of the energy flux of the electron-photon component in EAS does not depend strongly on the shower size. (We were not able to check this relation experimentally since the hodoscope detected showers with $N \lesssim 3 \times 10^5$ only.)

3. Bursts detected by a large-area array. For the selected events, whenever an axis of an EAS fell upon the array, we constructed the spectrum of the ionization bursts detected over the total area of the chamber layers underneath the 60 g/cm^2 graphite absorber. The burst size was then determined as the sum of the ionization in all chambers of a given layer. In addition, to increase the accuracy, we added the bursts in the two lower chamber layers. The spectrum of the bursts produced by the nuclear-active particles in EAS obtained in such a way using an array with a 10 m^2 area is shown in Fig. 3 (light circles). 596 showers were used to construct the spectrum. It can be seen that, in the burst-size range under consideration $6 \times 10^{12} \leq I_{na} \leq 10^5$, the burst spectrum cannot be described by a power law with a single exponent γ . The exponent varies from $\gamma \sim 0.8$ for small bursts ($I_{na} = 10^3 - 10^4$) to $\gamma = 1.3 - 1.4$ for large bursts ($I_{na} = 10^4 - 10^5$).

An analogous result was obtained at sea level. The spectrum of bursts (based on 128 showers) detected over the total area of the array at sea level is shown in Fig. 4. Here, too, the spectrum exponent varies from $\gamma \sim 0.7 - 0.8$ for bursts between 10^3 and 10^4 particles to $\gamma \sim 1.3$ for bursts greater than 10^4 .

The results concerning the spectrum exponent of bursts produced by nuclear-active particles in EAS in a large-area array are thus consistent with other experiments.

4. Variation of the burst spectrum with the array

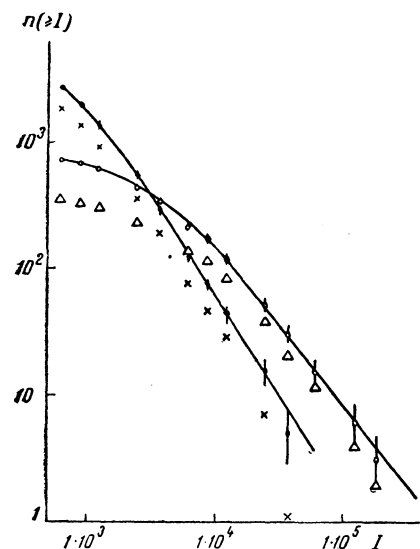


FIG. 3. Integral burst spectrum produced by nuclear-active particles in EAS at 3200 m above sea level. \circ, Δ - burst spectrum recorded over the total area of the array; \bullet, \times - burst spectrum in separate chambers. The spectrum Δ, \times refers to the 292 events with shower size (according to the hodoscope) greater than 10^5 particles.

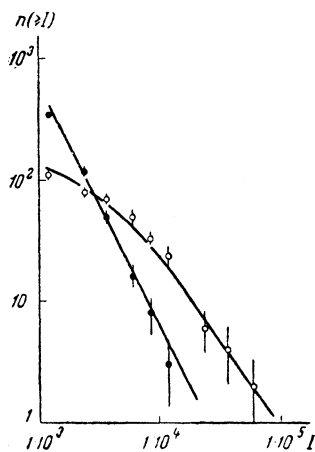


FIG. 4. Spectrum of bursts produced by nuclear-active particles in EAS at sea level (notation as in Fig. 3).

area. We were able to analyze large ionization bursts under 60 g/cm^2 graphite absorber since our array consisted of a large number of ionization chambers with a relatively small diameter and which could detect the bursts independently.

It was found that practically all bursts in the detected showers ($\geq 90\%$), greater than 3×10^3 particles, were due to the incidence of groups of nuclear-active particles upon the array. An example is shown in Fig. 1. It can be seen that the burst of $\sim 3 \times 10^4$ particles is due to a simultaneous incidence of a cascade of nuclear-active particles, consisting of ten or more particles. The conclusion about the presence of groups of nuclear-active particles in the core region of EAS is confirmed by the data of other authors. Thus, e.g., Vernov et al^[1] reported that in showers with $N \sim 5 \times 10^5$ there are, on the average, about 10 nuclear-active particles producing bursts of $I_{na} \geq 2 \times 10^3$, and all the particles propagate near the axis within a circle with a radius of 1 to 2 m. It is therefore very probable that an array with an area of the order of a square meter will detect several nuclear-active particles and, consequently, the burst spectrum measured by such an array does not correspond to the energy spectrum of nuclear-active particles.

It is evident that the smaller the dimensions of the array, the less probable is a simultaneous incidence of several particles upon it, and the better the fit between the spectrum of ionization bursts and the energy spectrum of nuclear-active particles. In order to decrease the detection probability of particle groups we constructed the spectrum of bursts detected by separate chambers with an area of $10 \times 330 \text{ cm}^2$ each. As it has been shown earlier,^[5] such a reduction of the data gives a result which most closely approaches the true spectrum of nuclear-active particles.

The spectrum was constructed for 596 selected showers with $N \geq 10^5$ particles ($I_{ep} \geq 1.2 \times 10^4$), using the bursts detected in each chamber of the two lower layers under the 60 g/cm^2 graphite absorber. To increase the accuracy, the spectra obtained for separate chambers were added together. The burst spectrum obtained in such a way from separate chamber measurements is shown in Fig. 3 (black points). It can be seen that it differs considerably from the burst spectrum detected over the total area of the array (10 m^2). While the latter is characterized by an exponent varying from $\gamma \sim 0.8$ to $\gamma = 1.3-1.4$, the exponent of the burst spectrum detected by single chambers has the same spectrum exponent $\gamma = 1.6 \pm 0.1$ over the whole range of burst sizes from 10^3 to 2×10^4 particles. It should be mentioned once more that both spectra are based on the same shower sample.

The burst spectrum in separate chambers at sea level is shown in Fig. 4. In the burst range $I_{na} = 10^3-10^4$ the spectrum has an exponent $\gamma = 2.0 \pm 0.2$, i.e., differs considerably from the burst spectrum detected over the whole area of the array.

To check whether the difference in the spectra is not due to a small number of showers with $N < 10^5$ present among the selected showers, we carried out a similar analysis of the bursts accompanied by EAS detected by the hodoscope. We chose 292 events in which the core of EAS fell upon the array, and for which the shower size was, according to the hodoscope indications, greater than 10^5 particles. The burst spectrum for the total area of the array (triangles) and for separate chambers (crosses) is shown for these showers in Fig. 3. It can be seen that the spectra are practically the same as for all events with $I_{ep} \geq 1.2 \times 10^4$ particles.

Thus the results obtained both at mountain altitude and at sea level indicate that the burst spectrum in separate ionization chambers and, consequently, the spectrum of nuclear-active particles in EAS, differ considerably from the burst spectrum detected by an array with a large working area and, in particular, from the spectra obtained in^[1,2].

In order to investigate the variation of the burst spectrum measured by separate chambers with the shower size \bar{N} we divided all the showers into four groups according to the burst size I_{ep} , detected in the upper chamber layer. Group I consists of showers which produced bursts from 1.2×10^4 to 3.6×10^4 particles (521 showers). The mean shower size determined from the hodoscope read-

ings is $\bar{N} = 1.5 \times 10^5$. The remaining groups were: group II — $3.6 \times 10^4 \leq I_{ep} \leq 1.2 \times 10^5$ particles ($\bar{N} = 5 \times 10^5$, 197 showers), group III — $1.2 \times 10^5 \leq I_{ep} \leq 3.6 \times 10^5$ particles ($\bar{N} = 1.5 \times 10^6$, 57 showers), group IV — $3.6 \times 10^5 \leq I_{ep} \leq 1.2 \times 10^6$ particles ($\bar{N} = 5 \times 10^6$, 20 showers). (It should be mentioned that in order to improve the statistics, especially for large showers, we included showers obtained in a selective reduction of additional experimental material. The number of showers in the groups does not represent therefore the true shower-size distribution.)

For each of the groups we constructed the integral spectrum of bursts detected by separate chambers of the lower layers. The spectra are shown in Fig. 5. The x axis represents the size of the ionization bursts in separate chambers of the lower layers, and the y axis the probability of observing,

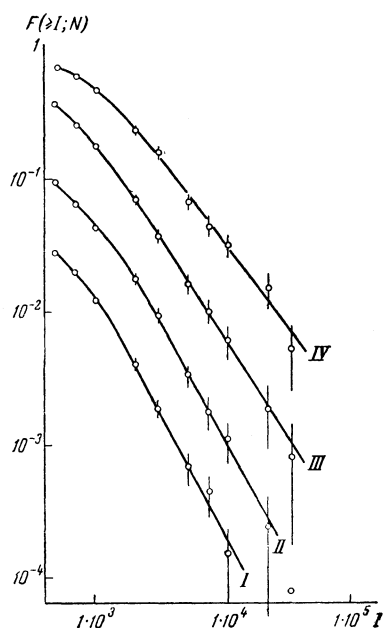


FIG. 5. Spectrum of bursts produced by nuclear-active particles in separate chambers for showers of different size.

in a separate chamber, a burst of a given value for an EAS core incident upon the array. In the burst range from 10^3 to 10^4 particles (for showers of group IV in the range from 10^3 to 3×10^4 particles) the spectra obtained can be represented by a power law with exponents $\gamma_I = 1.9$, $\gamma_{II} = 1.8$, $\gamma_{III} = 1.5$, and $\gamma_{IV} = 1.3$. All these spectra, including the burst spectrum from nuclear-active particles of the fourth shower group, are steeper than the burst spectrum detected over the total area of the array.

The fact that the burst spectrum in separate chambers becomes steeper with increasing shower size \bar{N} and the spectrum exponent γ decreases might be due to the following effect: the number of

nuclear-active particles incident simultaneously upon the array increases with increasing \bar{N} , as it follows from Fig. 5. For the showers of group I ($\bar{N} = 1.5 \times 10^5$), the detection probability for a single chamber of a burst with size greater than 10^3 particles is ~ 0.012 per shower. Since in the lower layers there were 32 chambers, then for EAS with $\bar{N} = 1.5 \times 10^5$ the mean frequency of bursts greater than 10^3 particles was $\sim 0.012 \times 32 \approx 0.4$ per shower. For the showers of group IV ($\bar{N} \approx 5 \times 10^6$) the frequency of such bursts amounted to ~ 16 per shower, i.e., the bursts with a size $I_{na} \geq 10^3$ particles will be observed on the average in 16 chambers of each of the lower layers underneath the 60 g/cm^2 graphite absorber. This means that for such showers a considerable ionization is observed in roughly half of the chambers of the lower layers (see Fig. 1) and that many nuclear-active particles fall simultaneously on the array. There is then a high probability that even separate chambers will be hit by several nuclear-active particles, which causes a decrease in the spectrum exponent γ . The energy spectrum of nuclear-active particles in EAS can, therefore, be characterized only by a larger exponent γ than the one found for the burst spectrum in separate chambers.

CONCLUSIONS

The data obtained indicate that the spectrum of bursts with $I_{na} \geq 10^3$ particles produced by nuclear-active particles in EAS depends considerably on the size of the detecting array. This is due to the fact that the particles producing such bursts propagate at small distances (one to two meters) from the shower axis, and that the average number of such particles per shower is large. When using an array with an area of the order of a square meter, several nuclear-active particles often hit simultaneously the detectors near the core of the EAS. As a result, the ionization-burst spectrum differs considerably from the spectrum of nuclear-active particles.

The burst spectrum in the range from 10^3 to 10^4 particles in showers with $N \sim 10^5 - 10^6$, measured using an array with a small working area, is characterized by a spectrum exponent $\gamma = 1.8 - 1.9$ while the burst spectrum detected by a large-area array has $\gamma = 1.0 - 1.4$ for the same burst-size range.^[1,2] The burst spectrum detected over the total area of our array also has an exponent γ considerably smaller than $1.8 - 1.9$.

The energy spectrum of nuclear-active particles in EAS corresponding to bursts greater than 10^3

particles can only be softer (i.e., have a greater exponent γ) than the burst spectrum measured in separate chambers. This is due to two facts: firstly it may happen that sometimes, especially for large showers, a single chamber will be hit by several nuclear-active particles; secondly, the results obtained by us refer to the core region of EAS only, as we detected nuclear-active particles propagating at a distance of 1 to 2 m from the shower axis. It is known that the mean distance at which nuclear-active particles can be deflected from the shower axis increases with decreasing particle energy. The smaller the energy of a nuclear-active particle (the smaller the burst produced by it), the greater the probability that it will miss the array and escape detection. The number of small bursts ($I_{na} \lesssim 10^3$ particles) in our spectrum may, therefore, be underestimated.

As a result, the exponent of the spectrum of nuclear-active particles in EAS can only be greater than the exponent of the burst spectrum measured in separate chambers. Accordingly, we should expect that in EAS with $N \sim 10^5-10^6$ particles the integral energy spectrum of nuclear-active particles producing bursts in the range from 10^3 to 10^4 particles (according to our estimates this corresponds to the energy range of nuclear-active particles $E \sim 5 \times 10^{11}-5 \times 10^{12}$ eV) can be represented by a power law with exponent $\gamma = 1.8-1.9$, and not $\gamma = 1$ as was found in [1,2].

¹ Vernov, Goryunov, Dmitriev, Kulikov, Nechin, and Khristiansen, Proc. IUPAP Conf. Cosmic Rays, Moscow, vol. 2, p. 123, 1960.

² Dovzhenko, Zatsepin, Murzina, Nikol'skiĭ, and Yakovlev, Proc. IUPAP Conf. Cosmic Rays, Moscow, Vol. 2, p. 144, 1960.

³ J. Tanaka, J. Phys. Soc. Japan 16, 5 (1961).

⁴ Babetski, Buya, Grigorov, Loskevich, Massal'skiĭ, Oles, and Shestoperov, JETP 40, 1551 (1961), Soviet Phys. JETP 13, 1089 (1961).

⁵ Babayan, Boyadzhyan, Grigorov, Tret'yakova, and Shestoperov, JETP 44, 22 (1963), Soviet Phys. JETP 17, 15 (1963).

⁶ V. A. Dmitriev, JETP 35, 553 (1958), Soviet Phys. JETP 8, 382 (1959).

⁷ Babecki, Buya, Grigorov, Loskevich, Massal'skiĭ, Oles, Shestoperov, and Fisher, JETP 41, 13 (1961), Soviet Phys. JETP 14, 8 (1962).

⁸ Vernov, Goryunov, Dmitriev, Kulikov, Nechin, Solov'eva, Strugal'skiĭ, and Khristiansen, Proc. IUPAP Conf. Cosmic Rays, Moscow, Vol. 2, p. 117, 1960.

⁹ Chudakov, Nesterov, Zatsepin, and Tukish, Proc. IUPAP Conf. Cosmic Rays, Moscow, Vol. 2, p. 47, 1960.

¹⁰ Kameda, Maeda, and Toyoda, Proc. IUPAP Conf. Cosmic Rays, Moscow, Vol. 2, p. 56, 1960.

Translated by H. Kasha